Catalysis Communications 99 (2017) 43–48

Contents lists available at ScienceDirect

Catalysis Communications

journal homepage: www.elsevier.com/locate/catcom

Short communication

Increased selectivity for allylic oxidation of cyclohexene using TiO_2 modified V_2O_5/MoO_3 catalysts

Guoqiang Yang[a], Matthew D. Huff[b], Huiyuan Du[a], Zhibing Zhang[a,*], Yu Lei[b,*]

[a] School of Chemistry and Chemical Engineering, Nanjing University, Nanjing, Jiangsu 210093, China
[b] Department of Chemical and Materials Engineering, University of Alabama in Huntsville, Huntsville, AL 35899, USA

ARTICLE INFO

Keywords:
Cyclohexene
Allylic oxidation
Epoxidation
Atomic layer deposition
Mixed metal oxides
Zeolite

ABSTRACT

V_2O_5 and MoO_3 mixed oxides supported by SiO_2 were studied as the catalysts in the aqueous phase allylic oxidation of cyclohexene to unsaturated alcohol 2-cyclohexene-1-ol and unsaturated ketone 2-cyclohexene-1-one. The additional layer of TiO_2 deposited by atomic layer deposition significantly suppresses the epoxidation pathway and the formation of cyclohexane oxide and cyclohexane-1, 2-diol. X-ray diffraction (XRD), X-ray photoelectron spectroscopy (XPS), and transmission electron microscopy (TEM) were used to study the relationship between the structure of the catalysts and their catalytic performance. The effects on the catalytic activity of different solvent, hydrogen peroxide to cyclohexene ratio, and reusability were investigated.

1. Introduction

The addition of oxygen to hydrocarbons is one of the simplest methods to manufacture value-added chemicals. Oxidation of hydrocarbons to epoxides, alcohols, aldehydes, and acids is a large category of catalytic organic reactions. For example, the oxidation of cyclic olefin, such as cyclohexene (C_6H_{10}, **(1)**), produces several oxygenated derivatives of great industrial interests, as shown in Scheme 1 [1]. As a model compound, cyclohexene **(1)** is particularly interesting as it has two active groups in the molecule, namely the C—H bond at the allylic site and the C=C bond. In the epoxidation pathway, the C=C bond is oxidized leading to formation of cyclohexane oxide **(2)** and a subsequent hydration product cyclohexane-1,2-diol **(3)**. In the allylic oxidation pathway, the C—H bond is attacked, resulting in formation of α,β unsaturated alcohol and ketone, namely 2-cyclohexene-1-ol **(4)** and 2-cyclohexene-1-one **(5)**. Both pathways are industrially important. The epoxidation pathway could eventually lead to the formation of adipic acid ($((CH_2)_4(COOH)_2)$), a chemical intermediate with high market demand [2,3]. The α, β unsaturated alcohol and ketone generated via allylic oxidation pathway are important intermediates in the fragrance industry and industrial organic synthesis [4]. Besides the industrial significance, understandings of the selective oxidation of cyclohexene could potentially help to design next generation catalysts for direct oxidation of hydrocarbons with two or more active groups.

MoO_3-based catalysts have been regarded as active catalysts for selective oxidation of hydrocarbons [5,6]. Particularly, Mo^{6+}/Mo^{5+} pairs are considered catalytic centers where Mo^{6+} oxo-peroxo species catalyzes the oxidation reaction and is simultaneously reduced to Mo^{5+} [5,7]. The Mo^{5+} can be subsequently oxidized back to Mo^{6+} oxo-peroxo species by oxygen sources such as O_2 and H_2O_2 [8]. The replenishing process can potentially benefit from the presence of vanadium oxides. When heated, the surface vanadium oxides can be re-dispersed to isolated VO_4 active sites [9]. These site isolated VO_4 species is known to help to replenish the oxygen vacancies. The synergistic effects between MoO_3 and V_2O_5 enable highly active catalysts for selective oxidation reactions [10,11].

Titanium silicalite-1 (TS-1) is commercially used to catalyze propylene to propylene oxide [12]. The presence of site-isolated Ti sites is believed important to improve the propylene epoxidation selectivity. Similarly, studies show that the presence of Ti sites favors the direct epoxidation pathway for selective oxidation of cyclohexene [13]. However, the selectivity could be affected by composition of materials and operation conditions. For example, high local concentration of H_2O_2 near Ti sites could lead to allylic oxidation pathway [14]. In other studies, Ti-grafted mesoporous silica catalysts favored allylic oxidation pathway. This study will focus at the effect of Ti in promoting V_2O_5-MoO_3/SiO_2 for selective oxidation of cyclohexene.

Atomic layer deposition (ALD) is a thin film deposition technique [15]. Taking advantages of surface self-limiting reactions, it enables conformal coatings of nanoparticles and thin films on high surface area supports with atomic precision. This feature makes it a promising tool to precisely synthesize advanced heterogeneous catalysts with well-controlled structure [16,17]. In this work, we used TiO_2 ALD to modify the surface the SiO_2 support. The presence of TiO_2 significantly

* Corresponding authors at: Department of Chemical and Materials Engineering, University of Alabama in Huntsville, Huntsville, AL 35899, USA.
E-mail addresses: zbzhang@nju.edu.cn (Z. Zhang), yu.lei@uah.edu (Y. Lei).

http://dx.doi.org/10.1016/j.catcom.2017.05.023
Received 28 March 2017; Received in revised form 21 May 2017; Accepted 22 May 2017
Available online 23 May 2017

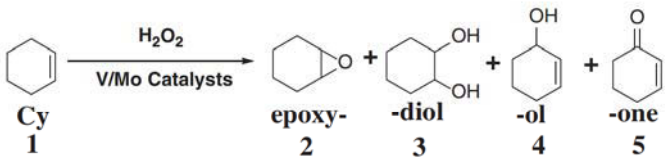

Scheme 1. Catalytic oxidation of cyclohexene.

suppressed the formation of cyclohexene oxide, leading to its selectivity decreased from 21% to 1.7%. This results in an increase in the selectivity to unsaturated alcohol and ketone from 67% to 48% at similar cyclohexene conversion.

2. Experimental

2.1. Catalyst preparation

Silicycle S10040M SiO_2 with a surface area of ~100 m^2/g was used as the catalyst support. TiO_2 ALD was performed by a viscous flow benchtop reactor (Gemstar-6, Arradiance) as described previously [18]. One ALD cycle of TiO_2 was deposited at temperatures of 200 °C using alternating exposure to titanium isopropoxide (TTIP, Sigma-Aldrich, 99.999%) and deionized water. In this work, the resulting TiO_2 modified SiO_2 is represented as $1cTiO_2/SiO_2$. The growth rate of TiO_2 ALD is ~0.3 Å/cycle which corresponds to an estimated ~4 wt% loading of TiO_2 on SiO_2 [19].

Deposition of V_2O_5-MoO_3 composite oxide nanomaterials were carried out by hydrothermal deposition on SiO_2 and $1cTiO_2/SiO_2$ as supports, respectively. 1.7421 g (1.410 mmol) $(NH_4)_6Mo_7O_{24}{\cdot}4H_2O$ (Sigma-Aldrich, 99.98%) and 0.1027 g (0.878 mmol) NH_4VO_3 (Sigma-Aldrich, 99.996%) were added to 50 mL of deionized water and the suspension was dissolved under stirring. After dissolved, stirring was continued for additional 15 min. Afterward, all 50 mL of the aqueous solution was added into 3 g of either the $1cTiO_2/SiO_2$ or SiO_2, and mixed again for 15 min in order to make the support is very well covered with aqueous solution. As a result, the as-prepared catalysts contain 1 wt% V_2O_5 and 24 wt% MoO_3. Finally, the suspension was put in furnace at 100 °C for 19.5 h, and the solid powder was immediately calcined at 600 °C for 3 h. The as-prepared sample was sealed in a capped glass vail in the dark for further analysis or use.

2.2. Catalyst characterization

Transmission electron microscope (TEM) images and energy dispersive x-ray spectroscopy (EDX) were obtained with a JEM-200CX microscope operated at 100 kV. The specimens for TEM were prepared by ultrasonically suspending the sample in acetone and depositing a drop of the suspension onto a grid. X-ray photoelectron spectroscopy (XPS) was performed in a PHI 5000 VersaProbe spectrometer equipped with an Al Kα X-ray source in ultrahigh vacuum (UHV) ($< 10^{-10}$ Torr). Binding energies (± 0.2 eV) were referenced to the C 1s peak at 284.6 eV as graphite. X-ray diffraction (XRD) patterns were recorded on a Rigaku MiniFlex 600 powder X-ray diffractometer equipped with a rotating anode using Cu K_α radiation (40KV, 15 mA). The Fourier transform infrared (FT-IR) spectra of the samples were recorded on a ThennoNicolet NEXUS870 FT-IR instrument (KBr discs) in the 4000–400 cm^{-1} region.

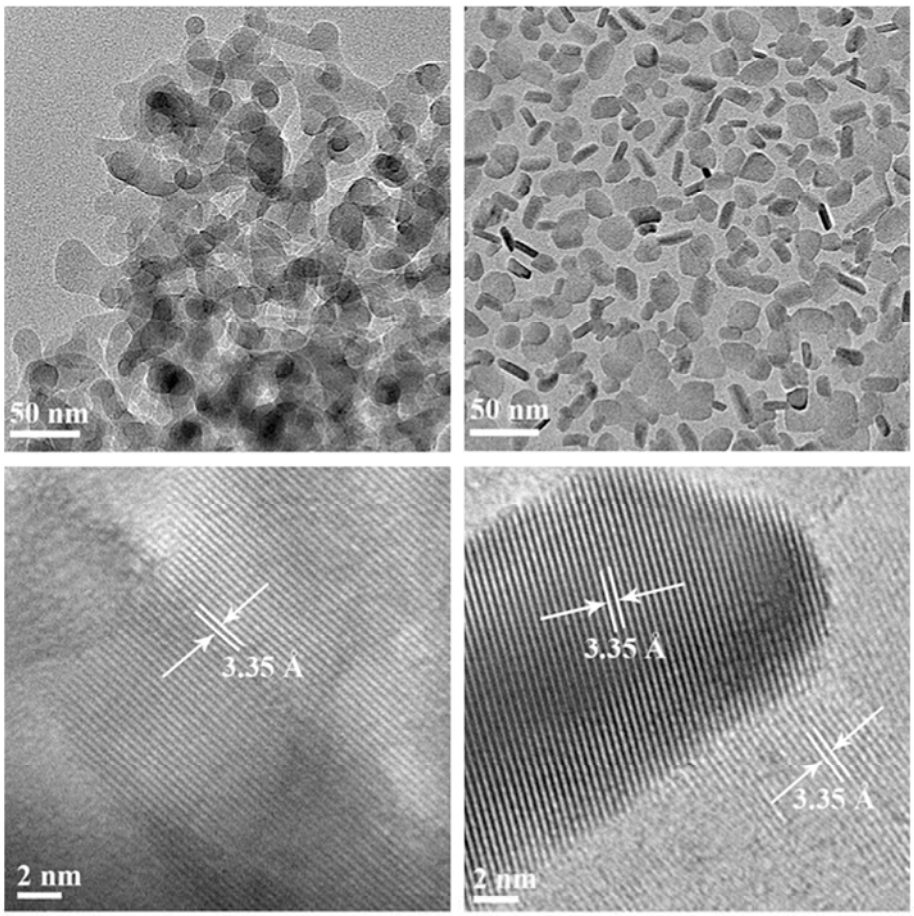

Fig. 1. TEM (up, left) and HRTEM (down, left) images of V_2O_5-MoO_3@SiO_2. TEM (up, right) and HRTEM (down, right) images of V_2O_5-MoO_3@($1cTiO_2/SiO_2$).

2.3. Catalyst activity test

The liquid phase catalytic oxidation of cyclohexene was carried out in a magnetically stirred round-bottom flask (25 mL) connected to a reflux condenser. 5 mmol of cyclohexene, 10 mL of acetonitrile, 0.5 mmol of o-dichlorobenzene (o-DCB) as internal standard, and 10 mg of catalyst were placed into the glass flask. The reaction was initiated by adding 30 wt% H_2O_2 solution with vigorous stirring. The quantitative analysis of reactants and products was performed on a Shimadzu GC2014 gas chromatograph equipped with a WondaCAP-5 capillary column (5% Diphenyl 95% Dimethylpolysiloxane 30 m × 0.32 mm × 0.25 μm) with a flame-ionization detector. A Shimadzu GCMS-QP2010 was used to identify substrates and their oxidation products resulting from catalysis. Cyclohexane oxide, cyclohexane-1,2-diol, 2-cyclohexene-1-ol and 2-cyclohexene-1-one are identified as major oxidation products. Other byproducts include adipaldehyde, 2,3-epoxycyclohexanol and 2,3-epoxycyclohexanone. Pristine SiO_2, TiO_2/SiO_2, and titanium silicalite (TS-1) were tested under reaction conditions as control experiments. The cyclohexene conversion was negligible. In the reusability measurements, the spent catalysts were recycled using high-speed centrifugation, washed by diethyl ether, and dried at 60 °C overnight.

3. Results and discussion

3.1. Catalyst characterization

Fig. 1 shows the HR-TEM images of V_2O_5-MoO_3@SiO_2 and V_2O_5-MoO_3@(TiO/SiO_2) catalysts, respectively. For V_2O_5-MoO_3@SiO_2 catalyst, spherical shape MoO_3 nanoparticles of ~13.2 nm in diameter are supported by SiO_2 gel. Due to the higher *Z*-number, MoO_3 appears to be darker spheres. The HR-TEM images show clear crystalline structure of MoO_3 with a plain distance of 3.35 Å, consistent with the (021) facet of MoO_3. Interestingly, for V_2O_5-MoO_3@(TiO/SiO_2) catalysts, the MoO_3 appears in the shape of nanorod with a length of ~20.8 nm and width of ~6.4 nm. The surface of the nanorod also shows a fringe of ~3.35 Å, similar to what was observed to MoO_3 in the V_2O_5-MoO_3@SiO_2 catalysts. EDX measurements were carried out on both catalysts to qualitatively determine the purity of the samples (please see Fig. S1 in the Supplemental Information (SI)). While there were V, Mo, Ti and Si in V_2O_5-MoO_3@(TiO/SiO_2) catalysts, only V, Mo and Si were detected in V_2O_5-MoO_3@SiO_2 catalysts. There was no other impurity presence in the as-prepared catalysts.

The purity of the sample was further confirmed using XPS survey scans (please see Fig. S2 in the SI). The elements observed in each sample were consistent with the EDX results. Fig. 2 and Table 1 compared the Mo 3d spectra obtained from the as-prepared and spent samples. Mo $3d_{5/2}$ and $3d_{3/2}$ spin-orbit splitting of doublets were observed in Mo 3d XPS spectra. The difference in binding energy between the doublets is 3.1 eV which matches well with the literature values for Mo oxides [20]. In the as-prepared catalysts, only one component appears at binding energies of Mo $3d_{5/2}$ peak at 232.9 eV and commonly assigned to Mo^{6+} species in octahedral coordination. The used V_2O_5-MoO_3@SiO_2 catalysts have three components which can be ascribed to Mo^{5+} species (232.3 eV), Mo^{6+} species in an octahedral coordination (233.0 eV), and Mo^{6+} species in tetrahedral coordination (233.6 eV). With the additional of TiO_2, the used V_2O_5-MoO_3@(TiO/SiO_2) catalysts only have two components which are Mo^{5+} species (232.3 eV) and Mo^{6+} species in the octahedral coordination (233.0 eV). During the allylic oxidation reaction, both catalysts were partially reduced from Mo^{6+} to Mo^{5+}. The Mo^{5+} components accounts for 68.3% and 71.3% of the molybdenum species in the used V_2O_5-MoO_3@SiO_2 and V_2O_5-MoO_3@(TiO/SiO_2), respectively. The presence of Mo^{6+}/Mo^{5+} pairs is consistent with the literature where the pairs are considered as catalytic centers.

V $2p_{3/2}$ and $2p_{1/2}$ spin-orbit splitting of doublets were observed with a difference in binding energy of 7.6 eV (please see Fig. S3 in SI). The as-prepared catalysts have two components of vanadium, i.e., V^{5+} (518.0 eV) and V^{4+} (517.0 eV) [21]. The V^{5+}:V^{4+} ratio is about 1:1 in the as-prepared catalysts. Due to the low loading of vanadium and possible leaching during the allylic oxidation reaction, the signal-to-noise of vanadium XPS spectra of the used catalysts is not sufficient to

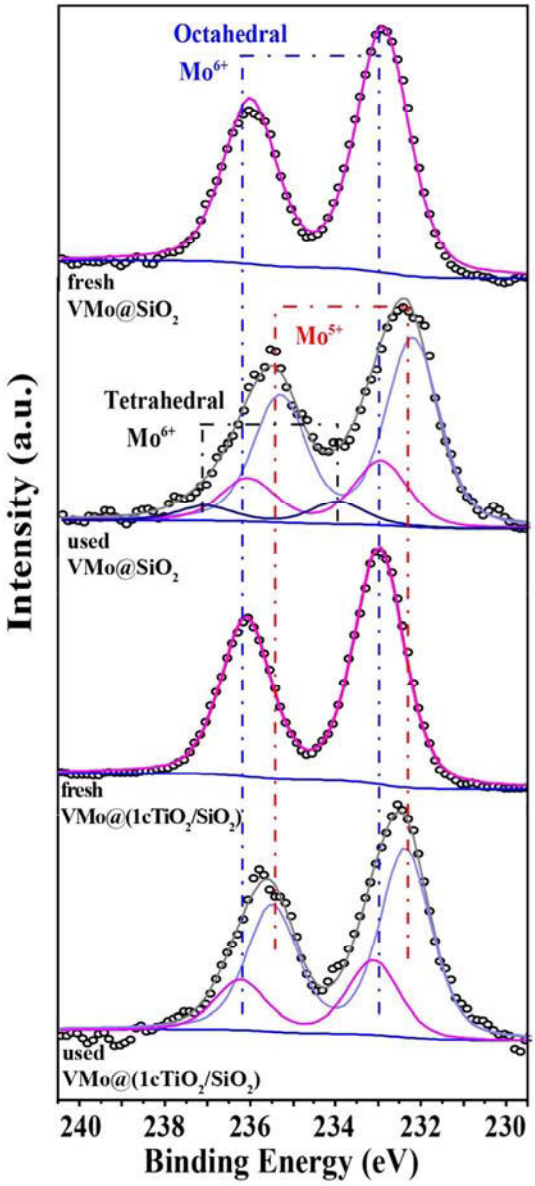

Fig. 2. Mo 3d XPS spectra of the fresh and used catalysts.

Table 1
The binding energies of Mo $3d_{5/2}$ and V $2p_{3/2}$ excitation.

	VMo@SiO_2 BE (eV)	VMo@(TiO_2/SiO_2) BE (eV)	VMo@SiO_2 used BE (eV)	VMo@(TiO_2/SiO_2) used BE (eV)	
Mo $3d_{5/2}$	–	–	232.3	232.4	Mo^{5+}
	232.9	232.9	233.0	233.1	Octahedral Mo^{6+}
	–	–	233.6	–	Tetrahedral Mo^{6+}
V $2p_{3/2}$	518.0	518.0	–	–	V^{5+}
	517.0	517.0	–	–	V^{4+}

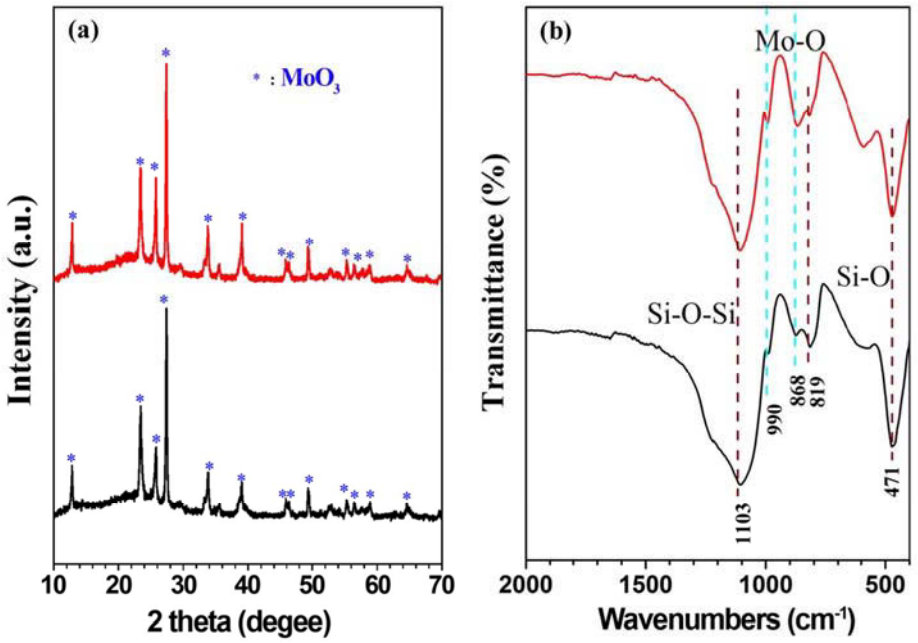

Fig. 3. (a) XRD patterns and (b) FT-IR spectra of the catalysts. *Red line*: V_2O_5-MoO_3@(1cTiO_2/SiO_2). *Black line*: V_2O_5-MoO_3@ SiO_2. (For interpretation of the references to colour in this figure legend, the reader is referred to the web version of this article.)

provide meaningful discussion, and therefore the spectra are not presented.

XRD was used to probe the structure of the as-prepared catalysts. The as-prepared catalysts contain α-MoO_3 structure, as shown in Fig. 3a, which matches well with the XPS data fittings. Fig. 3b shows several features determined using FT-IR spectroscopy. Two features can be ascribed to the presence of SiO_2, including the Si—O—Si stretch vibration mode (1103 cm^{-1}) and Si—O—Si rocking mode (471 cm^{-1}) [22]. The feature at 868 cm^{-1} is likely the symmetric stretching mode of Mo—O—Mo and the Si—O—Si bending mode. The feature at 819 cm^{-1} is attributed to the stretching mode of vibration of asymmetric bridging oxygen in Mo—O—Mo [23]. The feature at 990 cm^{-1} is assigned to the Mo═O characteristic stretching vibration of α-MoO_3 [24]. The loading of vanadium and titanium were probably too low to be distinguished from the IR features of SiO_2 and MoO_3.

3.2. Catalyst performance evaluation

Reaction conditions such as the choice of solvent, reaction temperature, quantity of catalysts in use, hydrogen peroxide to cyclohexene ration were optimized by carrying a series of controlled experiments. Table S1 shows the results obtained by testing nine different solvents, including acetone (CH_3COCH_3), methanol (CH_3OH), ethanol (CH_3CH_2OH), acetonitrile (CH_3CN), dichloromethane (CH_2Cl_2), chloroform ($CHCl_3$), tetrahydrofuran ($(CH_2)_4O$, THF), benzonitrile (C_6H_5CN), and water (H_2O). The non-polar solvent chloroform favored the formation of cyclohexene oxide. The polar protic solvents (methanol, ethanol, and water) resulted in high selectivity to *α, β* unsaturated alcohol or ketone and the selectivity to cyclohexene oxide decreased with increasing solvent dielectric constant (DC). However, neither non-polar nor polar protic solvents were ideal solvents for selective oxidation of cyclohexene as they suffered from lower cyclohexene conversion (1%–2%). Polar aprotic solvents in general offered higher cyclohexene conversion as compared to non-polar and polar protic solvents. However, the reaction pathway seemed independent of dielectric constant of the polar aprotic solvents. While dichloromethane (DC = 9.1) and benzonitrile (DC = 26.0) favored the formation of cyclohexene oxide, other polar aprotic solvents (DC = 7.5–37.5) resulted in the formation of *α, β* unsaturated alcohol or ketone. In terms of reaction activity, highest conversion (11%) was achieved when acetonitrile was used as the solvent. Therefore, acetonitrile was chosen as the solvent for the rest of the study due to its 94% combined selectivity towards *α, β* unsaturated alcohol and ketone and a relative high conversion.

The proper reaction temperature was determined by evaluating the catalysts in temperature range from 35 °C to 75 °C with 10 °C interval (please see Fig. S4). The conversion increases with increasing reaction temperature. After 10 h, the conversion of the reaction at 75 °C almost reaches 100% while the conversion at 35 °C is only 24%. In terms of selectivity, high temperature favors epoxidation pathway forming epoxy and diol and low temperature favors allylic oxidation pathway forming *α, β* unsaturated alcohol and ketone. With increasing reaction temperature, the combined selectivity to 2-cyclohexene-1-ol and 2-cyclohexene-1-one gradually decreased from 83% at 35 °C to 23% at 75 °C. Particularly, at 75 °C the selectivity to cyclohexane-1,2-diol increases significantly to 58% with minimal cyclohexane oxide. It implies that high temperature favors epoxidation pathway and significantly improves the reaction rate of the subsequent hydration to form cyclohexane-1,2-diol. As a result, a reaction temperature of 55 °C was chosen to carry out future catalyst evaluations due to its relatively high conversion and combined selectivity to 2-cyclohexene-1-ol and 2-cyclohexene-1-one.

The proper amount of catalyst used in the reaction was evaluated 55 °C, as shown in Fig. S5. The conversion of cyclohexene is negligible when no catalyst is added. The conversion increases with increasing the amount of catalyst from 0 mg to 20 mg. However, the conversion decreases when the amount of catalyst further increases. The conversion decrease is probably because the catalyst starts to effectively accelerate the disproportionation of H_2O_2 into O_2 and H_2O. In addition, the selectivity to cyclohexane-1,2-diol increases from 10% to 34% when the amount of catalyst increases from 5 mg to 40 mg. As a consequence, 10 mg–20 mg catalysts were determined to be the proper quantity of catalysts to be used in the reaction.

The effect of H_2O_2 was studied by varying the H_2O_2/cyclohexene ratio from 0.5, 1, 1.5 to 2.0 (please see Fig. S6). Under H_2O_2 poor condition (H_2O_2: cyclohexene = 0.5: 1), the combined selectivity to 2-cyclohexene-1-ol and 2-cyclohexene-1-one are 91% without any production of cyclohexane-1,2-diol. The selectivity to 2-cyclohexene-1-one

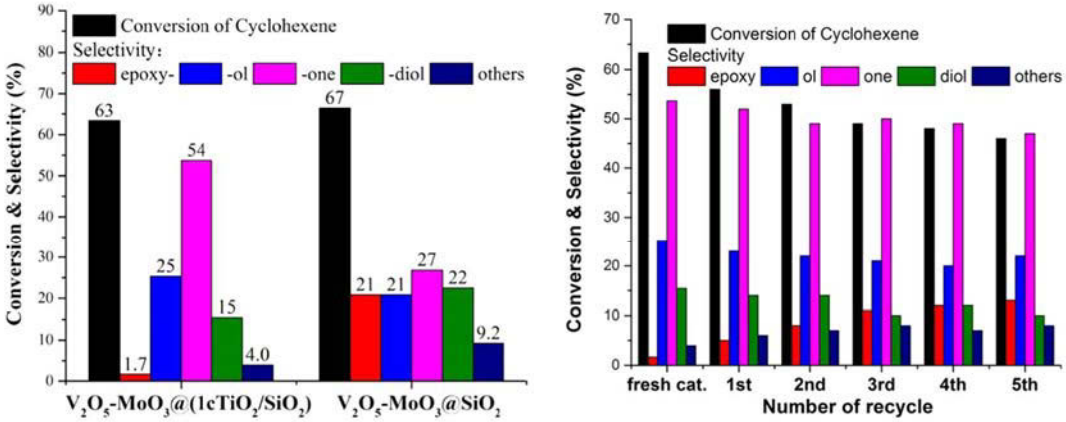

Fig. 4. Catalysts performance (left) and reusability (right). Reaction conditions: Cyclohexene 5 mmol, the molar ratio of hydrogen peroxide to cyclohexene is 1.5, catalyst 10 mg, acetonitrile 10 mL, 55 °C, 10 h. The catalyst was separated by centrifugation after the previous run, dried at 100 °C under vacuum and then subjected to the following run under the same conditions.

decreased with increasing H_2O_2 molar ratio of hydrogen peroxide to cyclohexene. Excess amount of H_2O_2 did not significantly cause formation of diol and other byproducts.

V_2O_5-MoO_3@SiO_2 and V_2O_5-MoO_3@(TiO/SiO_2) catalysts were then evaluated using the optimized reaction conditions determined by the controlled experiments. The results are shown in Fig. 4. The presence of TiO_2 significantly suppressed the epoxidation reaction and the formation of cyclohexene oxide, leading to decrease in selectivity from 21% to 1.7%. The lowering of cyclohexene oxide selectivity results in an increase in the selectivity to unsaturated alcohol and ketone from 48% to 79% at similar cyclohexene conversion. The presence of TiO_2 also decreases the selectivity to diol from 22% to 15% and selectivity to other byproducts from 9.2% to 4.0%.

The reusability of the V_2O_5-MoO_3@(TiO/SiO_2) catalysts were tested for five times. The conversion of cyclohexene gradually decreases from 63% at the initial entry to 46% at the fifth recycle, and the selectivity to cyclohexane oxide increases from 2% to 13%. This is probably due to the leaching of active components such as TiO_2 during the reaction and recycling process, which was observed in previous studies [14,25]. Because of the possible TiO_2 leaching during each entries, the composition of V_2O_5-MoO_3@(1cTiO_2/SiO_2) catalyst gradually became similar to the unmodified V_2O_5-MoO_3@SiO_2 catalyst, causing the reaction pathway shifted from allylic oxidation to epoxidation.

The behavior of V_2O_5-MoO_3@SiO_2 catalyst with and without TiO_2 ALD coating is very different. According to these preliminary results, it appears that the TiO_2-modified V_2O_5-MoO_3@SiO_2 catalyst does not alter the reactivity but significantly suppresses the epoxidation reaction pathway. Work is in progress to elucidate these differences and overcome the challenge of materials leaching during the reaction.

4. Conclusions

Selective oxidation of cyclohexene was investigated for SiO_2 supported V_2O_5-MoO_3 mixed oxide catalysts. It is feasible to tune the reaction pathway between epoxidation and allylic oxidation by the choice of solvents. Under the conditions studied in this work, low temperature, low H_2O_2/cyclohexene ratio, and small quantity of catalyst in use favors allylic oxidation pathway. Upon modification of the SiO_2 surface with one ALD cycle of TiO_2, the V_2O_5-MoO_3@(1cTiO_2/SiO_2) catalyst showed good activity in allylic oxidation of cyclohexene compared with its unmodified counterpart V_2O_5-MoO_3@SiO_2. The epoxidation pathway is largely suppressed with the presence of TiO_2 on the SiO_2 surface, resulting in increased selectivity to the unsaturated alcohol and ketone, namely 2-cyclohexene-1-ol and 2-cyclohexene-1-one. Catalyst leaching from V_2O_5 and TiO_2 decreases both the conversion and the selectivity to the allylic oxidation products.

Acknowledgements

G. Yang, H. Du, and Z. Zhang gratefully acknowledge the grants from the National Natural Science Foundation of China (No. 21476105). M. Huff and Y. Lei acknowledge the National Science Foundation (Grant# CBET-1511820) for the financial support.

Appendix A. Supplementary Data

Supplementary data to this article can be found online at http://dx.doi.org/10.1016/j.catcom.2017.05.023.

References

[1] S. Van de Vyver, Y. Roman-Leshkov, Emerging catalytic processes for the production of Adipic acid, Catal. Sci. Tech. 3 (2013) 1465–1479.
[2] K. Weissermel, H.-J. Arpe, Industrial Organic Chemistry, fourth ed., WILEY-VCH, Weinheim, Germany, 2003.
[3] K. Sato, M. Aoki, R. Noyori, A "green" route to adipic acid: direct oxidation of cyclohexenes with 30 percent hydrogen peroxide, Science 281 (1998) 1646–1647.
[4] Y. Cao, H. Yu, F. Peng, H. Wang, Selective allylic oxidation of cyclohexene catalyzed by nitrogen-doped carbon nanotubes, ACS Catal. 4 (2014) 1617–1625.
[5] J. Dou, F. Tao, Selectie epoxidation of cyclohexene with molecular oxygen on catalyst of nanoporous au integrated with MoO_3 nanoparticles, Appl. Catal. A 529 (2017) 134–142.
[6] J. Dou, H.C. Zeng, Integrated networks of mesoporous silica nanowires and their bifunctional catalysis-sorption application for oxidative desulfurization, ACS Catal. 4 (2014) 566–576.
[7] M. Conte, X. Liu, D.M. Murphy, S.H. Taylor, K. Whiston, G.J. Hutchings, Insights into the reaction mechanism of cyclohexane oxidation catalysed by molybdenum blue nanorings, Catal. Lett. 146 (2016) 126–135.
[8] D.V. Deubel, G. Frenking, P. Gisdakis, W.A. Herrmann, N. Rosch, J. Sundermeyer, Olefin epoxidation with inorganic peroxides. Solutions to four long-standing controversies on the mechanism of oxygen transfer, Acc. Chem. Res. 37 (2004) 645–652.
[9] T. Kim, I.E. Wachs, CH_3OH oxidation over well-defined supported V_2O_5/Al_2O_3 catalysts: influence of vanadium oxide loading and surface vanadium-oxygen functionalities, J. Catal. 255 (2008) 197–205.
[10] Y. Meng, T. Wang, S. Chen, Y. Zhao, X. Ma, J. Gong, Selective oxidation of methanol to dimethoxymethane on V_2O_5-MoO_3/γ-Al_2O_3 catalysts, Appl. Catal. B 160–161 (2014) 161–172.
[11] M. Faraldos, M.A. Banares, J.A. Anderson, H. Hu, I.E. Wachs, J.L.G. Fierro, Comparison of silica-supported MoO_3 and V_2O_5 catalysts in the selective partial oxidation of methane, J. Catal. 160 (1996) 214–221.
[12] S.J. Khatib, S.T. Oyama, Direct oxidation of propylene to propylene oxide with molecular oxygen: a review, Catal. Rev. Sci. Eng. 57 (2015) 1–39.
[13] G. Lapisardi, F. Chiker, F. Launay, J.P. Nogier, J.L. Bonardet, A "one-pot" synthesis of adipic acid from cyclohexene under mild conditions with new bifunctional Ti-AlSBA mesostructured catalysts, Catal. Commun. 5 (2004) 277–281.
[14] J.M. Fraile, J.I. Garcia, J.A. Mayoral, E. Vispe, Effect of the reaction conditions on the epoxidation of alkenes with hydrogen peroxide catalyzed by silica-supported titanium derivatives, J. Catal. 204 (2001) 146–156.
[15] S.M. George, Atomic layer deposition: an overview, Chem. Rev. 110 (2010) 111–131.
[16] M. Lu, R.B. Nuwayhid, T. Wu, Y. Lei, K. Amine, J. Lu, Atomic layer deposition for lithium-based batteries, Adv. Mater. Interfaces 3 (2016) 1600564.

[17] J. Lu, J.W. Elam, P.C. Stair, Atomic layer deposition-sequential self-limiting surface reactions for advanced catalyst "bottom-up" synthesis, Surf. Sci. Rep. 71 (2016) 410–472.
[18] M. Piernavieja-Hermida, Z. Lu, A. White, K.-B. Low, T. Wu, J.W. Elam, Z. Wu, Y. Lei, Towards ALD thin film stabilized single-atom Pd_1 catalysts, Nano 8 (2016) 15348–15356.
[19] Y. Lei, B. Liu, J. Lu, J.A. Libera, J.P. Greeley, J.W. Elam, Effects of chlorine in titanium oxide on palladium atomic layer deposition, J. Phys. Chem. C 118 (2014) 22611–22619.
[20] M. Zimowska, K. Latka, D. Mucha, J. Gurgul, L. Matachowski, The continuous conversion of ethanol and water mixtures into hydrogen over Fe_xO_y/MoO_3 catalytic system-XPS and mossbauer studies, J. Mol. Catal. A Chem. 423 (2016) 92–104.
[21] G. Silversmit, D. Depla, H. Poelman, G.B. Marin, R. De Gryse, Determination of the V2p XPS binding energies for different vanadium oxidation states (V^{5+} to V^{0+}), J. Electron Spectrosc. Relat. Phenom. 135 (2004) 167–175.
[22] G. Das, L. Ferraioli, P. Bettotti, F. De Angelis, G. Mariotto, L. Pavesi, E. Di Fabrizio, G.D. Soraru, Si-nanocrystals/SiO_2 thin films obtained by pyrolysis of sol–gel precursors, Thin Solid Films 516 (2008) 6804–6807.
[23] C.S. Caetano, I.M. Fonseca, A.M. Ramos, J. Vital, J.E. Castanheiro, Esterification of free fatty acids with methanol using heteropolyacids immobilized on silica, Catal. Commun. 9 (2008) 1996–1999.
[24] C. Li, Q. Xin, K. Wang, X. Guo, FT-IR emission spectroscopy studies of molybdenum oxide and supported molybdena on alumina, silica, zirconia, and titania, Appl. Spectrosc. 45 (1991) 874–882.
[25] U. Schuchardt, D. Cardoso, R. Sercheli, R. Pereira, R.S. da Cruz, M.C. Guerreiro, D. Mandelli, E.V. Spinace, E.L. Pires, Cyclohexane oxidation continues to be a challenge, Appl. Catal. A 211 (2001) 1–17.